# Comparison of a Three-Phase Single-Stage PV System in PSCAD and PowerFactory

Afshin Samadi, Robert Eriksson, Della Jose, Farhan Mahmood, Mehrdad Ghandhari and Lennart Söder
Department of Electric Power Systems
KTH Royal Institute of Technology
Stockholm, Sweden 10044
Email: afshin.samadi@ee.kth.se, robert.eriksson@ee.kth.se, mehrdad.ghandhari@ee.kth.se, lennart.soder@ee.kth.se

*Abstract*—**Accommodating more and more distributed PhotoVoltaic (PV) systems within load pockets has changed the shape of distribution grids. It is not, therefore, accurate anymore to address distribution grids just only as a lumped load. So it will be crucial in the near future to have an aggregate model of PV systems in distribution grids. By doing so, it is important to develop models for PV systems in different simulation platforms to study their behavior in order to derive an aggregate model of them. Although, there have been several detailed-switching model of a PV system in EMTDC/PSCAD simulation platform in literature, these non-proprietary switching models are slow in simulation, particularly when the number of the PV systems increases on the grounds that in PSCAD the simulation is based on time domain instantaneous values and requires more mathematical details of components. Therefore, in this paper a model of the PV system in DIgSILENT/PowerFactory is developed, which is a proper environment to run rms simulation and works based on the phasors and, moreover, from mathematical perspective is more simplified. The performance of the stemming model is compared with the switching model in PSCAD. Comparing the simulation results of the proposed model in PowerFactory with the model in PSCAD shows the credibility and accuracy of the proposed model.**
**Keywords: Photovoltaic, PSCAD, PowerFactory, Reactive power support**

## I. INTRODUCTION

High penetration of solar PhotoVoltaic (PV) systems has shaped a new structure for distribution grid. Growing trends in generating power from distributed PV systems have accommodated more and more PV systems in distribution grids. In Germany, for instance, there are currently 20 GW installed PV systems, of which 80% have been connected in low voltage grids [1]. This high penetration of PV systems has also raised new challenges in distribution grids such as voltage profile. Violation of voltage profile in some regions in Germany has led to stopping PV installation by utilities. To contrive a way to solve the unwanted problems associated with high penetration, several approaches have been proposed in recent standards and literature, for instance the reactive power support and the active power curtailment [2]–[5].

In power system studies, distribution grids have mainly been modeled as a lumped load. However it is not anymore wise to just address distribution grids as a passive load [6], [7]. The aforementioned changes that gradually happen in distribution grids require deeming new models of distribution grids for static and dynamic studies of power systems. Therefore, it is crucial to find a proper aggregate model of distribution grids consisting of PV systems in order to properly study the behavior of distribution grids on power system stability and dynamics.

In order to find out a suitable aggregate model of distributed PV systems, it is required to study the behavior of an individual PV system to discover how it functions in the grid. A power test system including PV systems is simulated either as a transient simulation, which uses instantaneous values, or an rms simulation which is based on the phasor model. In the transient simulation, components are needed to be modeled in more mathematical details; however, it, in turn, takes more simulation time. Although rms simulation of the PV system using phasor model is run faster, it excludes some mathematical details. Nevertheless, it is important to find out differences and similarities between these two simulation platforms and models, and then if the dynamic behavior of both models are similar, using phasor model is more time efficient and convenient in order to investigate and attain an aggregated model of distributed PV systems.

Models of a PV system in PSCAD have been addressed in literature such as [8]–[11]. Due to the old standards in the past, those models did not consider different reactive power strategies; however contemporary standards, e.g. German Grid Codes [12], allow reactive power support by PV systems. For instance, [8] only considers unity power factor operation and does not address the reactive power support; Ref. [9] does not consider Maximum Power Point Tracking (MPPT) and reactive power support; proposed model in [10] has been mainly developed for utility application and does not address different reactive power support strategies in distribution grids. Ref. [11] developed a model of a PV system which comprises four different reactive power supports and this model was incorporated in a test distribution grid with two PV systems. In this research a model of the PV system based on the proposed model in [11] is developed in PowerFactory for the rms simulation. There is already one developed generic PV model in PowerFactory Library, however this model has a few differences with the developed PSCAD model, for instance the standard MPPT function is not included and dc-link capacitor has been modeled through power equation. Therefore, since the main aim is comparing two identical models in a similar way, a new model is needed to be developed in PowerFactory.

The objective of this paper is to validate two identical models of a three-phase single-stage PV system in two different simulation platforms, namely PSCAD and PowerFactory, which perform simulations based on time domain instan-
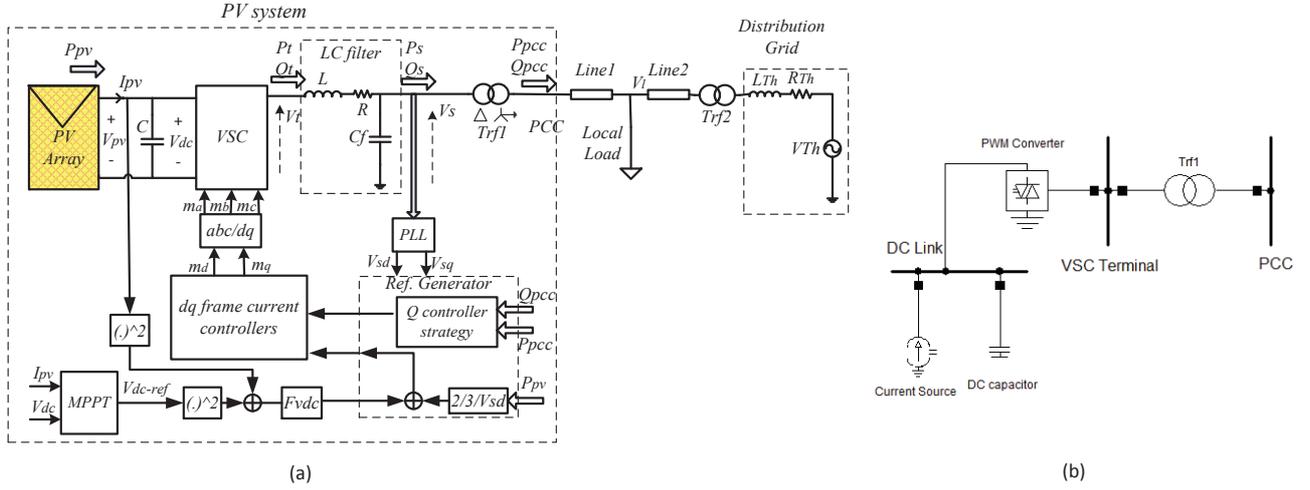
Figure 1. a) Schematic of a PV system structure connected to a distribution grid. b) Schematic of a PV system in PowerFactory.

taneous values and rms values, respectively. Four different reactive power support strategies have been incorporated into the models, i.e. fixed power factor, power factor as a function of feed-in power (hereinafter called dynamic power factor), reactive power depending the voltage Q(V), and AC-Bus voltage regulator. In conclusion, the both designed models are compared and simulation results demonstrate the credibility of those models; differences between them are shown and evaluated.

In the following, a general overview of PV systems structure will be given in section 2, differences and similarities between two models are presented in section 3, section 4 presents results of comparison of a single PV system connected to grid in the both simulation platforms and finally the conclusion comes at section 5.

## II. PV SYSTEMS STRUCTURE

Fig. 1 illustrates the one-line diagram schematic of a three pahse single-stage PV system connected through a transformer to a distribution grid. The PV system consists of PV array, dc-link capacitor, Voltage Source Converter (VSC) and peripheral control systems.

Solar cells are connected in series to form PV modules and PV modules are, in turn, connected in series or in parallel to form PV panels. PV panels are connected in series and in parallel to form solar array in order to provide adequate power and voltage for being connected to a grid. The output power of PV array feeds in dc-capacitor link which is connected in parallel and is transformed through parallel connected VSC to AC power. The VSC terminals are connected to the Point of Common Coupling (PCC) via the interface reactor, shown by L and R, and a transformer. The transformer makes an isolated ground for PV system as well as boosting the level of output voltage of PV system to the grid voltage level. $C_f$ is the shunt capacitor filter that absorbs undesirable low-frequency current harmonics generated by PV system. Distribution grid is assumed by Thevenin model where $R_{Th}$ and $L_{Th}$ are equivalent grid resistance and inductance, respectively.

Control system is performed in a dq-frame reference. Phase Locked Loop (PLL) is used to synchronize control

system with the grid frequency by moving from the abc-frame reference to a proper dq-frame reference.

### A. PV array model

Analogous with a diode, PV panel current-voltage characteristic is exponential and is depicted as follows:

$$I = I_{ph} - I_0 \left( exp \left( \frac{V - R_s I}{V_T} \right) - 1 \right) \tag{1}$$

In (1), I and V are output current and voltage of a PV panel respectively, $I_o$ is the dark saturation current, $R_s$ is the cell series resistance, $I_{ph}$ is the photo-generated current and $V_T$ is the junction thermal voltage. Ref. [13] shows how to calculate solar panel parameters $R_s$, $I_o$ and $I_{ph}$ by means of datasheet values in Standard Test Condition (STC). $I_{ph}$, short circuit current and open circuit voltage of the panel are linearly dependent on the irradiance and the temperature, while $I_o$ is only the temperature-dependent [13].

As mentioned earlier solar panels are connected in series and parallel, so the (1) can be extended as follows:

$$I_{pv} = n_p I_{ph} - n_p I_0 \left( exp \left( \frac{V_{pv} - R_s I_{pv}}{n_s V_T} \right) - 1 \right) \tag{2}$$

where $V_{pv}$ and $I_{pv}$ are PV array output voltage and current, and $n_s$ and $n_p$ are number of series and parallel panels, respectively.

### B. Controller model of PV system converter

Due to the different abc/dqo transformation, active power and reactive power are controlled on q and d axes in PSCAD, respectively, while it is the other way around in PowerFactory. Nevertheless, for integrity it is here assumed that active power is controlled on the d axis and reactive power on the q axis. Control system in a PV system on the each axis comprises two control loops where the inner loop is the current control (Fig. 2) and the outer loop is the dc-link voltage controller, which regulates active power, on the d axis and reactive power regulator on the q axis.

Active power control in PV systems is performed through regulating the dc-link voltage. The dc-link voltage regulator in the Laplace domain, $F_{vdc}(s)$, which in this study is an
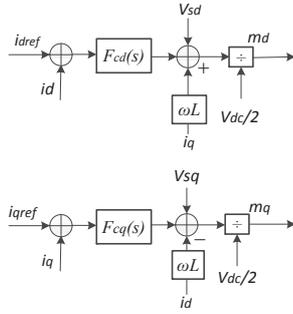
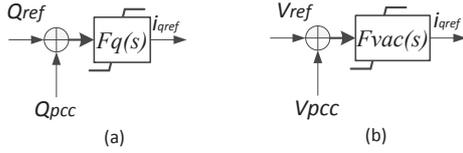Figure 2. Schematic of current control block diagram.



Figure 3. a) Block diagram of reactive power control loop. b) Block diagram of voltage control.
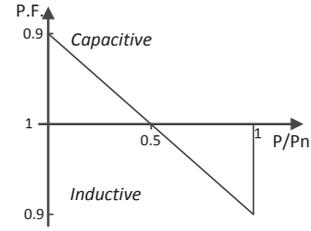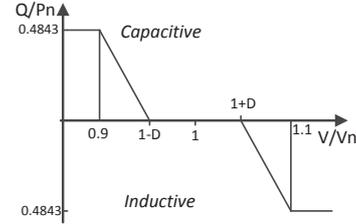


Figure 4. Dynamic power factor characteristic, PF(P).



Figure 5. Droop control strategy, Q(V).



Figure 6. Voltage-Power characteristic of a PV array for different irradiance levels.

integrator and a lead compensator, adjusts $i_{dref}$ through the dc-link voltage deviation signal ($\Delta V_{dc}$). In order to augment the performance of the dc-link voltage regulator, output power of PV can also be deployed as a feed-forward to eliminate the nonlinearity and the destabilizing impact of the PV array output power [9], [14].

Reactive power control can be done by different strategies. Nevertheless, from regulator design perspective it can be done either by regulating reactive power at a reference value (Fig. 3(a)) or controlling the voltage at the connection point to a set-point value (Fig. 3(b)). It must, however, be considered that the reactive power contribution of the PV system is limited according to the current standards [12]. Reactive power regulators, $F_q(s)$ or $F_{vac}(s)$, which in general can be a PI controller, adjust $i_{qref}$ using the reactive power deviation signal ($\Delta Q$) or the AC-bus voltage deviation signal ($\Delta V_{AC}$) depending on the reactive power control strategy. $\Delta i_d = i_{dref} - i_d$ and $\Delta i_q = i_{qref} - i_q$ are passed through current controllers to produce Sinusoidal Pulse Width Modulation (SPWM) signals for VSC in PSCAD.

Regarding reactive power contribution, a PV system could carry out this task through one of the following approaches:

I *Constant power factor operation*: PV system feeds reactive power into the grid irrespective of the voltage profile.
II *Dynamic power factor operation, PF(P)*: This method was proposed by German Grid Codes [12] (Fig. 4).
III *Droop-based control strategy, Q(V)*: This approach is a droop-based control strategy and Fig. 5 depicts a linear droop curve where the value of the dead-band (D) depends on the network impedance [15].
IV *Voltage control*: this approach is sensitive to the set-point adjustment to the extent that reactive power pumping interactions among PV systems in a distribution grid can occur [11].
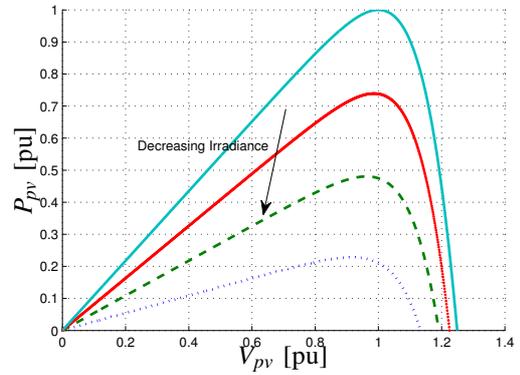
## C. MPPT of PV system

The energy captured from PV array is not only proportional to irradiance, but also depends upon the location of the operating point, in Fig. 6 it can be noticed. Therefore, the output of PV array is not necessarily equal to its maximum and by doing so, PV system always needs additional function to exploit maximum power of PV array which is named Maximum Power Point Tracking in literature. As can be seen in Fig. 1, MPPT determines the dc-link voltage reference. MPPT is actually the most outer control loop of the PV system that has a memory to provide the dc-link voltage reference by measuring the output voltage and current of PV arrays and comparing them with previous states through a processing algorithm. Here in this paper, Incremental Conductance (INC) [16] algorithm is employed.

## III. DIFFERENCES AND SIMILARITIES

In PSCAD, active power is controlled on the q axis and reactive power on the d axis due to abc/dq transformation characteristic. However, in PowerFactory the d axis represents the active power control and the q axis represents

| PV system parameter | Value |
|---|---|
| Vmp panel voltage at mpp | 33.7 V |
| Imp panel current at mpp | 3.56 A |
| Isc panel short circuit current | 3.87 A |
| Voc panel open circuit voltage | 42.1 V |
| Panel temperature coef. of Isc | 0.065 %/$^oC$ |
| Panel temperature coef. of Voc | -160 mV/$^oC$ |
| $n_s$ num. of series panels | 14 |
| $n_p$ num. of parallel panels | 6 |
| DC link capacitor C | 10 mF |
| Interface reactor L | 4 mH |
| Interface reactor R | 3 mΩ |
| Trf1 rated power | 15 kVA |
| Trf1 voltage ratio | 0.38/0.18 kV |
| MPPT frequency | 20 Hz |
| MPPT perturbation size | 0.337 V |
| Line Parameter | Value |
| Line1 impedance | 6 + 7.5j mΩ |
| Line2 impedance | 15.5 + 3.4j mΩ |
| Grid Parameter | Value |
| Grid voltage | 20 kV |
| Grid short circuit capacity | 1.15 MVA |
| Grid R/X ratio | 0.6 |
| Trf2 rated power | 250 kVA |
| Trf2 voltage ratio | 0.38/0.18 kV |
| Load Parameter | Value |
| Rated active power | 0.6 kW |
| Rated reactive power | 0.3 kVar |
| Rated voltage | 20 kV |
| Controller Parameter | Value |
| $F_{Vdc}=\frac{k}{s}\times\frac{1+sT_1}{1+sT_2}$ | k=8.65e3 A/V/s $T_1$=0.0232 $s^{-1}$ $T_2$=0.0011 $s^{-1}$ |
| $F_{cc}=k_{pcc}+\frac{k_{icc}}{s}$ | $k_{pcc}$=8Ω $k_{icc}$=2Ω/s |
| $F_q=k_{pq}+\frac{k_{iq}}{s}$ | $k_{pq}$=-0.227 A/Var $k_{iq}$= -453.5 A/Var/s |



Figure 7.   Irradiance variation



Figure 8.   The dc-link voltage response to irradiance variations, without MPPT.

reactive power. In PowerFactory, PWM converter block contains the current control block internally and it is possible to enable or disable it. The current control in PSCAD as can be seen in Fig. 2 comprises of decoupled terms while in PowerFactory the model of the current control is different. Therefore, the built-in current control is disabled by setting all the controller parameters to zero. Moreover, series reactor has been also located inside the PWM converter block in PowerFactory while in PSCAD the reactor is outside the converter. MPPT function uses same INC algorithm in both models.

## IV. COMPARISON OF A SINGLE PV SYSTEM CONNECTED TO GRID IN THE BOTH SIMULATIONS PLATFORMS

Two models according to Fig. 1 are built in two simulation platforms, PSCAD and PowerFactory. The parameters of the system are presented in Table I.

An identical simulation scenario is carried out in order to make a fair and comprehensive comparison between two models. Fig. 7 depicts irradiance variations during simulation which varies stepwise for simplicity. Since PowerFactory starts simulation around one operating point while PSCAD simulates from scratch, the simulation are shown from the point that PSCAD has been settled down at the initial operating point for the both models, where irradiance is around 1000 W/$m^2$.
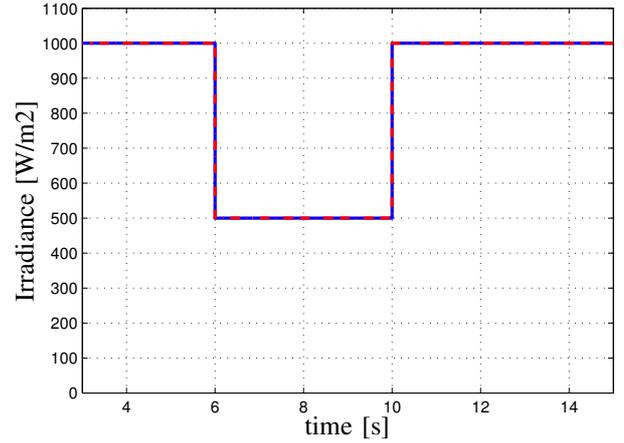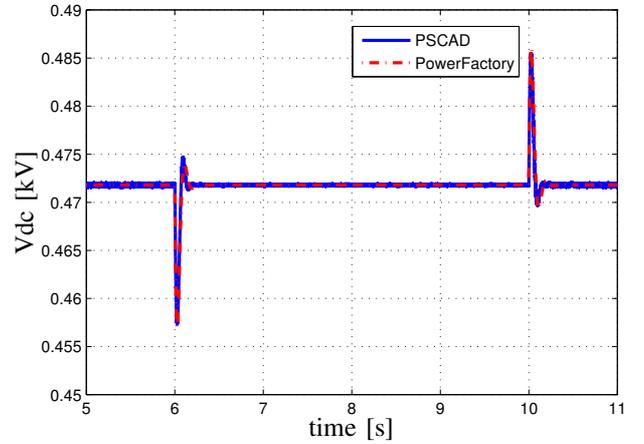
- *Case 1: Comparison without MPPT*

In this case study MPPT is disabled and dc-link voltage set-point $v_{dc-ref}$ is imposed by a constant value equal to 471.8 V which is the voltage at the maximum power point for irradiance equal to 1000 W/$m^2$. The objective of this section is only to compare the performance of both models from numerical solving perspective not showing the necessity of MPPT, therefore the dc-link voltage is regulated at the STC value. Fig. 8 demonstrates the dc-link voltage for both models followed by irradiance variation according to Fig. 7, and as it shows the dynamic performance of the both models are quiet similar. Fig. 9 depicts the output power of PV system, as can be seen the general dynamic response structures of the both models are same, with the same numbers of overshoot and undershoot, although the only difference is that the size of overshoot in PowerFactory model is a bit higher than PSCAD that might be due to the converter model in PowerFactory.

- *Case 2: Comparison with MPPT*

This case study is similar to the prior case study, except that the MPPT is enabled in this case study. Fig. 10 shows the dc-link voltage in PowerFactory model has more oscillatory transients than PSCAD. Although the
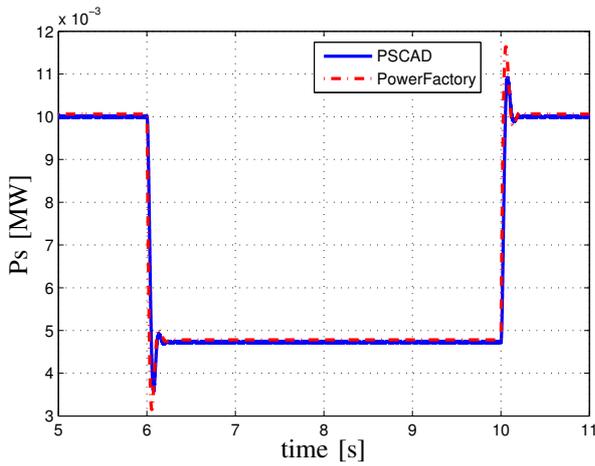
Figure 9. Active power response to irradiance variations, without MPPT.
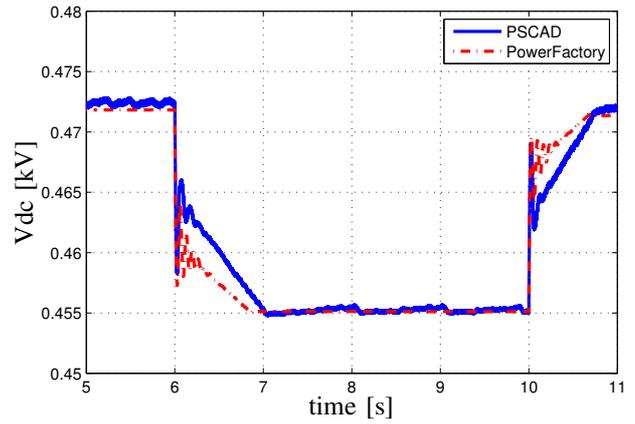


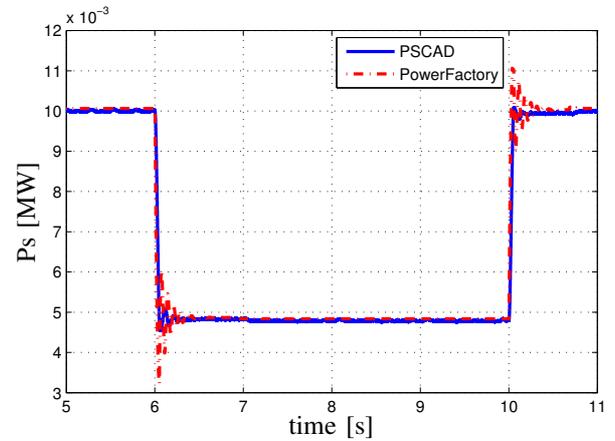Figure 10. The dc-link voltage response to irradiance variations, with MPPT.



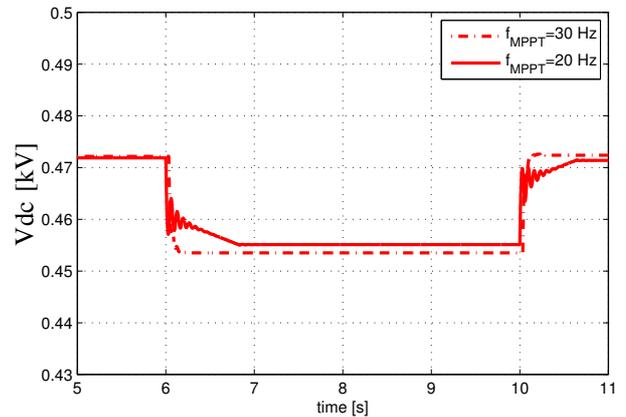Figure 11. Active power response to irradiance variations, with MPPT.



Figure 12. The dc-link voltage response to irradiance variations in PowerFactory for different MPPT frequencies.

same algorithm for implementing MPPT has been taken into consideration for the both models, the difference in the transient response might be owing to different solvers of software. At the steady-state stage, Power-Factory model shows no distortion around the operating point which can be due to the switching in PSCAD that makes confusion for the perturbation orientation in MPPT algorithm and so it leads to oscillations around MPP for the PV system in PSCAD. Fig. 11 depicts the output active power of the PV system and as can be seen the PowerFactory model response has more oscillatory transient with higher overshoot that could be expected from the result of the previous case study.

Increasing the MPPT frequency decreases oscillations, as Fig. 12 shows increasing the MPPT frequency to 30 decreases considerably oscillations. Although the final values of $V_{dc}$ in different frequencies are not the same, the difference is too small and it is due to the perturbation step and the design criterion in INC algorithm [16]. It boils down to this fact that once the PV system operating point goes close to MPP, the MPPT algorithm stops generating new perturbation as long as the absolute summation of the incremental conductance and the instantaneous conductance is smaller than a selective small value that is 0.001 in this study [16]. Furthermore, it is obvious that increasing the MPPT frequency increases noticeably the speed of the dc-link voltage response.

- Case 3: Different specification for dc-link voltage controller

  This case study is analogous with the previous case study, the only exception is the dc-link controller that has been designed for another specifications. In case 2 the specifications are 60 degree phase margin and 200 Hz bandwidth, but in this case study the phase margin is increased to 70 degree and bandwidth is also reduced to 130 HZ that is expected to get a slower system response. Figs. 13 and 14 show the dc-link voltage and active power, respectively. Although both models have more or less similar responses, the output power response of the PV system has higher overshoots and

undershoots. Apart from the models comparison, comparison of different design specifications shows that the performance of the PV system is considerably affected by changing dc-link specifications to the extent that in the second design, the PV system response becomes slower. Therefore, regarding making equivalent of PV systems in grid, one should deem this issue.
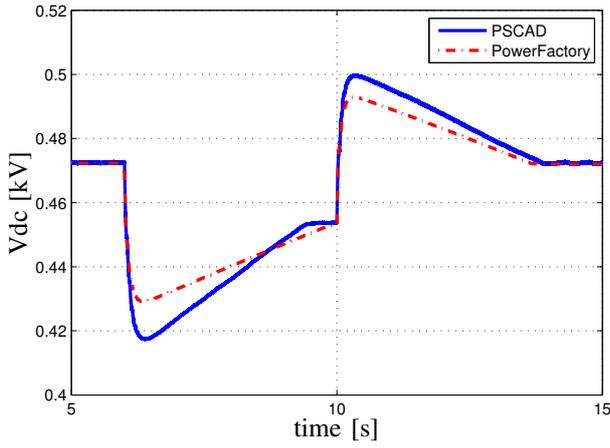
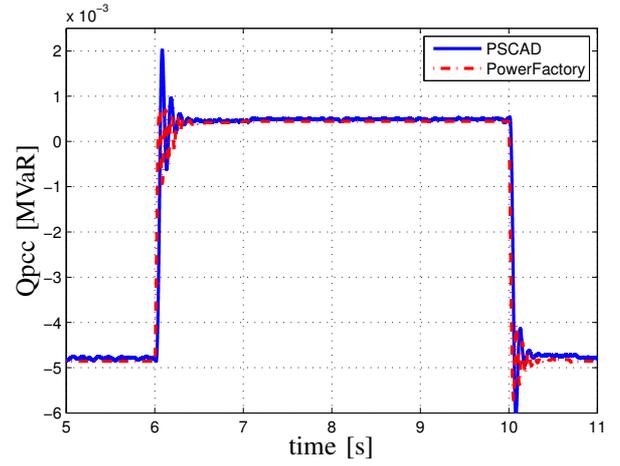Figure 13.  dc-link voltage response to irradiance variation, with MPPT.



Figure 14.  Active power response to irradiance variation, with MPPT.



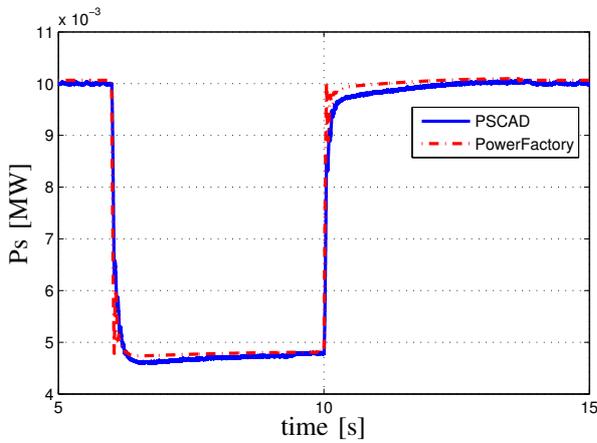Figure 15.  Reactive power at PCC, dynamic power factor strategy (II), with MPPT.
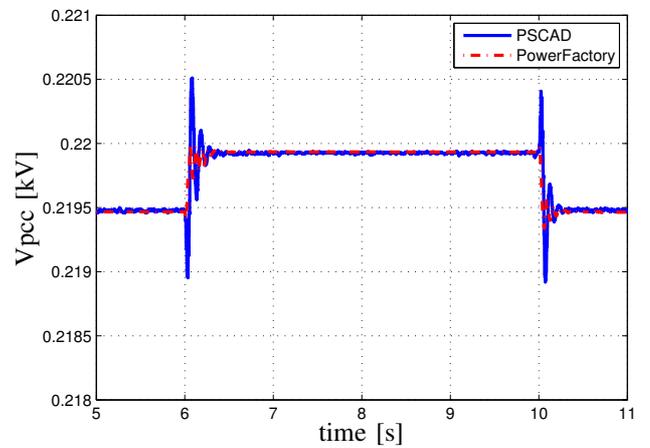


Figure 16.  The PCC voltage, dynamic power factor strategy (II), with MPPT.



Figure 17.  Reactive power at PCC, droop control strategy (III), with MPPT.

- *Case 4: Comparison reactive power strategies with MPPT*

  In this case study, the behavior of the PV system in both models, with the last three aforementioned reactive power strategies, is taken into account. Figs. 15 and 16 show reactive power at PCC and the PCC voltage for the dynamic power factor control (strategy II). The reactive power is less oscillatory in the PowerFactory model.

  For studying the droop-based reactive power control strategy (strategy III), a grid voltage incident is created by increasing 5 % the grid voltage at t=6 sec and return to its initial value after 1 sec while the irradiance remains constant at 1000 W/$m^2$. The droop parameter, D, in Fig. 5 is set to 0.03. Figs. 17 and 18 show the reactive power at PCC and the PCC voltage for droop-based reactive power control strategy, respectively.

  In the voltage control method (strategy IV), the voltage of the PCC is regulated to a desired set-point. The voltage set-point for the voltage control strategy is chosen according to the voltage at PCC once the PV system is connected to the grid and works with half of the nominal power. Figs. 19 and 20 show reactive power at PCC and the PCC voltage for voltage control strategy, respectively.
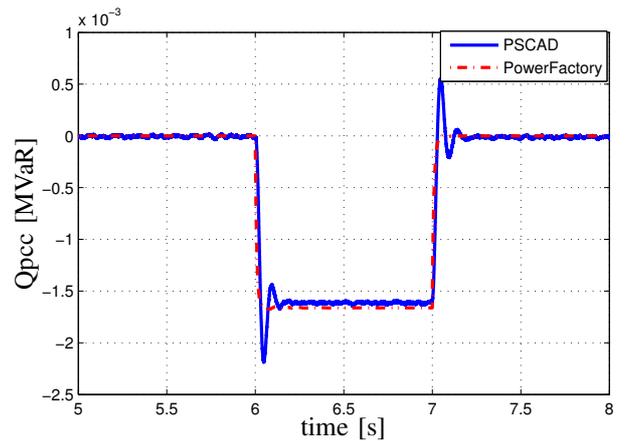
- *Case 5: Three-phase to ground fault with MPPT*

  This case study demonstrates the effect of the three-phase to ground fault on the PV system for the strategy IV. Irradiance is kept constant at 1000 W/$m^2$ and a fault incident is occurred at the load connection point
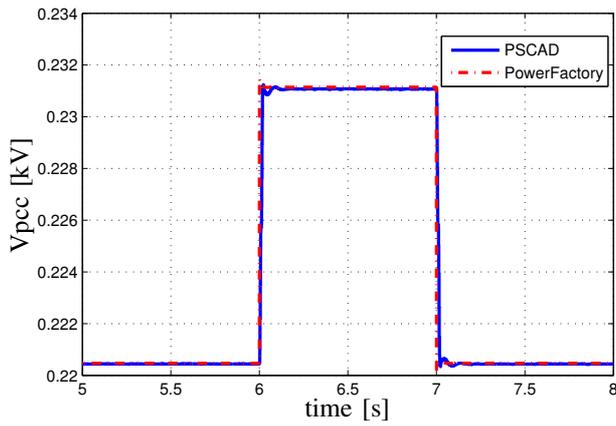
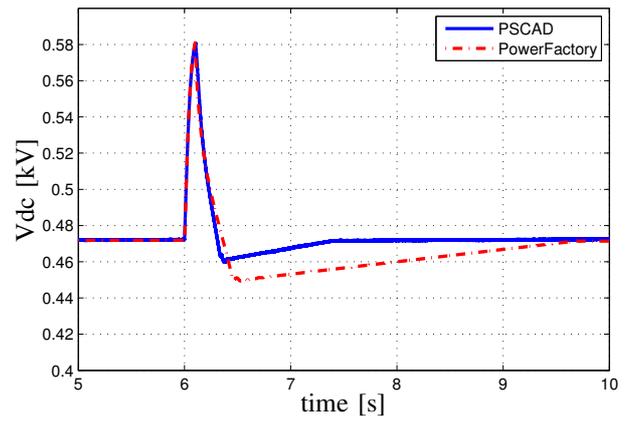Figure 18. The PCC voltage, droop control strategy (III), with MPPT.



Figure 19. Reactive power at PCC, voltage control strategy (IV), with MPPT.



Figure 20. The PCC voltage, voltage control strategy (IV), with MPPT.



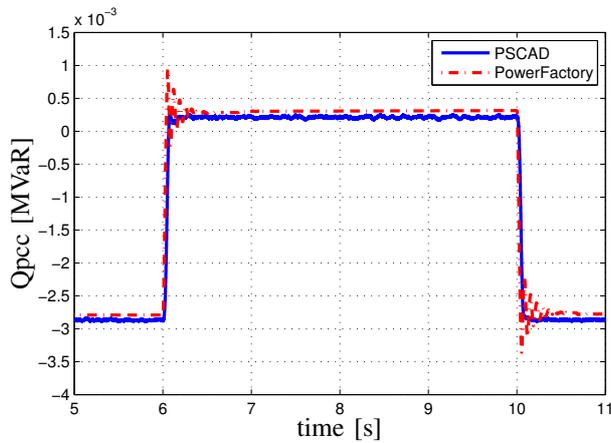Figure 21. dc-link voltage response to three-phase to ground fault, with MPPT.



Figure 22. PV active power response to three-phase to ground fault, with MPPT.

and reactive power of the PV system, respectively. As can be seen, the general trajectory of responses is the same in both models, however there are slight differences specially after fault clearance. The reactive power contribution during fault is too small. This is because of small active power that is provided by PV array to feed dc-link capacitor and it is, in turn, due to the PV output voltage that is shifted towards the open circuit voltage where the PV output power becomes zero.

## V. CONCLUSION

In this paper a model of a three-phase single-stage PV system was developed in PowerFactory platform. The performance of the developed was compared and confirmed with the PSCAD model, which was stemming from the previous research. The results show that both models are responding similarly to irradiance variation, although there are slight differences in the transient period subsequent to changes that might be due to MPPT function and numerical solving issues in the control system that are related to different solvers that are used in both software. Nevertheless, the results show that using rms values based simulations in PowerFactory

at t=6 s and cleared 100 ms later. The fault impedance is resistive and equal to 0.008 Ω. The dc-link bus voltage is shown in Fig. 21, as expected from power equation across the dc-link capacitor, the dc-link voltage is boosted. During fault interval, the transient behavior of both model are quiet similar. However, after fault clearance the transient response of both models have slight differences. Figs. 22 and 23 show active power
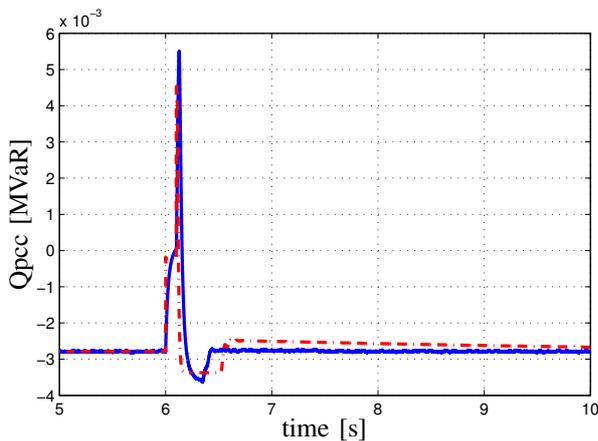
Figure 23. Reactive power at PCC, three-phase to ground fault, with MPPT.

can provide us with quite similar results using time domain instantaneous values. Therefore, the performance of large number of PV systems can be easily studied using rms simulations.

### REFERENCES

[1] J. C. Boeme and et al, "Overview of german grid issues and retrofit of photovoltaic power plants in germany for the prevention of frequency stability problems in abnormal system conditions of the ENTSO-E region continental europe," in *1st International Workshop on Integration of Solar Power into Power Systems*, (Aarhus, Denmark), pp. 3–8, Oct. 2011.

[2] M. Braun, "Reactive power supply by distributed generators," in *2008 IEEE Power and Energy Society General Meeting - Conversion and Delivery of Electrical Energy in the 21st Century*, pp. 1 –8, July 2008.

[3] P. Sulc, K. Turitsyn, S. Backhaus, and M. Chertkov, "Options for control of reactive power by distributed photovoltaic generators," *arXiv:1008.0878*, Aug. 2010. Proceedings of the IEEE , vol.99, no.6, pp.1063-1073, June 2011.

[4] R. Tonkoski, L. Lopes, and T. EL-Fouly, "Droop-based active power curtailment for overvoltage prevention in grid connected PV inverters," in *2010 IEEE International Symposium on Industrial Electronics (ISIE)*, pp. 2388 –2393, July 2010.

[5] E. Demirok, D. Sera, R. Teodorescu, P. Rodriguez, and U. Borup, "Evaluation of the voltage support strategies for the low voltage grid connected PV generators," in *2010 IEEE Energy Conversion Congress and Exposition (ECCE)*, pp. 710 –717, Sept. 2010.

[6] A. Ellis, M. Behnke, and J. Keller, "Model makers," *IEEE Power and Energy Magazine*, vol. 9, pp. 55 –61, June 2011.

[7] A. Ellis, M. Behnke, and C. Barker, "PV system modeling for grid planning studies," in *2011 37th IEEE Photovoltaic Specialists Conference (PVSC)*, pp. 002589 –002593, June 2011.

[8] S.-K. Kim, J.-H. Jeon, C.-H. Cho, E.-S. Kim, and J.-B. Ahn, "Modeling and simulation of a grid-connected PV generation system for electromagnetic transient analysis," *Solar Energy*, vol. 83, pp. 664–678, May 2009.

[9] A. Yazdani and P. Dash, "A control methodology and characterization of dynamics for a photovoltaic (PV) system interfaced with a distribution network," *IEEE Transactions on Power Delivery*, vol. 24, pp. 1538 –1551, July 2009.

[10] A. Yazdani, A. Di Fazio, H. Ghoddami, M. Russo, M. Kazerani, J. Jatskevich, K. Strunz, S. Leva, and J. Martinez, "Modeling guidelines and a benchmark for power system simulation studies of three-phase single-stage photovoltaic systems," *IEEE Transactions on Power Delivery*, vol. 26, pp. 1247 –1264, Apr. 2011.

[11] A. Samadi, M. Ghandhari, and L. Söder, "Reactive power dynamic assessment of a PV system in a distribution grid," *Energy Procedia*, vol. 20, pp. 98–107, 2012.

[12] "Verband der elektrotechnik elektronik Informationstechnike.V. (VDN) (2010). erzeugungsanlagen am niederspannungsnetz technische mindestanforderungen für anschluss und parallelbetrieb von erzeugungsanlagen am niederspannungsnetz. draft of 07-08-2010. berlin."

[13] D. Sera, R. Teodorescu, and P. Rodriguez, "PV panel model based on datasheet values," in *IEEE International Symposium on Industrial Electronics, 2007. ISIE 2007*, pp. 2392 –2396, June 2007.

[14] A. Yazdani and R. Iravani, *Voltage-Sourced Converters in Power Systems*. Wiley, 1 ed., Feb. 2010.

[15] G. Kerber, R. Witzmann, and H. Sappl, "Voltage limitation by autonomous reactive power control of grid connected photovoltaic inverters," in *Compatibility and Power Electronics, 2009. CPE '09.*, pp. 129 –133, May 2009.

[16] K. Hussein, I. Muta, T. Hoshino, and M. Osakada, "Maximum photovoltaic power tracking: an algorithm for rapidly changing atmospheric conditions," *Generation, Transmission and Distribution, IEE Proceedings-*, vol. 142, pp. 59 –64, Jan. 1995.